

1 **Adaption of a Conventional ELISA to a 96-well ELISA-Array for**
2 **Measuring the Antibody Responses to Influenza virus proteins,**
3 **viruses and vaccines**

4 **Eric Waltari^{1*}, Esteban Carabajal¹, Mrinmoy Sanyal², Natalia Friedland², Krista M.**
5 **M^cCutcheon¹**

6
7 ¹Chan Zuckerberg Biohub, San Francisco, CA, USA

8 ²Stanford ChEM-H and Department of Biochemistry, Stanford University School of Medicine,
9 Stanford, CA, USA

10

11 *** Correspondence:**

12 Eric Waltari

13 Eric.Waltari@czbiohub.org

14

15 **Keywords:** ELISA-Array, infectious disease, protein array, titer

16 **Abstract**

17 We describe an adaptation of conventional ELISA methods to an ELISA-Array format using
18 non-contact Piezo printing of up to 30 spots of purified recombinant viral fusion proteins,
19 vaccine and virus on 96 well high-protein binding plates. Antigens were printed in 1 nanoliter
20 volumes of protein stabilizing buffer using as little as 0.25 nanograms of protein, 2000-fold less
21 than conventional ELISA. The performance of the ELISA-Array was demonstrated by serially
22 diluting n=8 human post-flu vaccination plasma samples starting at a 1/1000 dilution and
23 measuring binding to the array of Influenza antigens. Plasma polyclonal antibody levels were
24 detected using a cocktail of biotinylated anti-human kappa and lambda light chain antibodies,
25 followed by a Streptavidin-horseradish peroxidase conjugate and the dose-dependent signal was
26 developed with a precipitable TMB substrate. Intra- and inter-assay precision of absorbance units
27 among the eight donor samples showed mean CVs of 4.8% and 10.8%, respectively. The plasma
28 could be differentiated by donor and antigen with titer sensitivities ranging from 1×10^3 to $4 \times$
29 10^6 , IC_{50} values from 1×10^4 to 9×10^6 , and monoclonal antibody sensitivities in the ng/mL
30 range. Equivalent sensitivities of ELISA versus ELISA-Array, compared using plasma and an
31 H1N1 HA trimer, were achieved on the ELISA-Array printed at 0.25ng per 200um spot and
32 1000ng per ELISA 96-well. Vacuum-sealed array plates were shown to be stable when stored for
33 at least 2 days at ambient temperature and up to 1 month at 4-8°C. By the use of any set of

34 printed antigens and analyte matrices the methods of this multiplexed ELISA-Array format can
35 be broadly applied in translational research.

36 **INTRODUCTION**

37 The activity of humoral antibodies provide the best correlation to long-term immune memory
38 and protection (Antia et al. 2018). During the first two weeks of exposure to a pathogen, the
39 majority of antibodies found in the serum derive from plasmablasts, either rapidly re-activated
40 from memory B cell pools or expanded from newly stimulated, somatically hypermutated and
41 differentiated B cells upon contact with antigen in lymph tissue (De Silva and Klein 2015).
42 During recovery, some plasmablasts will home to the bone marrow where they terminally
43 differentiate into long-lived plasma cells stably secreting antibodies that circulate in serum for
44 many years (Abbas, Lichtman, and Pillai 2014; Yoshida et al. 2010). Cellular and molecular
45 events leading to antigen-specific B cell expansion, differentiation, homing and fate are complex
46 and not predictable in outcome. In lieu, serum can be used to measure the binding kinetics,
47 magnitude, specificity and cross-reactivity of the secreted antibodies in response to infection or
48 vaccination. Serological testing can help evaluate an individual's susceptibility, exposure or
49 protection from past, existing and future pathogens. It is also possible to make positive or
50 negative correlations of binding characteristics to serum neutralization activity or antibody
51 enhanced disease (Katzelnick et al. 2017). Analytical methods characterizing antibodies ideally
52 have the ability to measure the robustness, specificity and genetic breadth of activity to
53 pathogens. Humoral responses are typically quantified by titer in naïve, acute, convalescent and
54 recovery sera in the context of natural infection or pre- and post- vaccination and correlated to *in*
55 *vitro* activity assays and clinical signs of immune protection (e.g. Antia et al., 2018; Lowell et
56 al., 2017; Madore et al., 2010).

57 The enzyme-linked-immunosorbent-assay (ELISA) first described by Engvall and
58 Perlmann (1972), is commonly used to measure specific antibody-antigen binding. Variants and
59 derivatives of the ELISA have become assay workhorses of immunology laboratories and a host
60 of compatible reagents, consumables, plate washers, multichannel pipettes, robotic liquid
61 handlers, and assay formats have been developed and are available from multiple vendors. A
62 conventional antigen ELISA single plex format passively coats antigens on a 96-well high

63 capacity protein binding surface (e.g. Nunc Maxisorp™, ThermoFisher Scientific, Waltham,
64 MA) and indirectly titers primary antibody binding by secondary binding of polyclonal
65 antibodies conjugated to horseradish peroxidase (HRP), which turns over the colorimetric
66 3,3',5,5'-tetramethylbenzidine (TMB) substrate for assay readout. Secondary antibodies are
67 typically directed against a constant region of the heavy or light chain of the primary antibody,
68 such as polyclonal anti-Fc directed to IgG, IgM, IgA or IgE, anti-kappa or anti-lambda light
69 chains. A common variation to boost sensitivity includes using a biotinylated secondary antibody
70 with a Streptavidin-horseradish peroxidase (HRP) conjugate. Although fluorescent reporters
71 have the advantage of allowing for multiplexed detection using different dyes, the use of HRP
72 has been shown to be more sensitive because the enzymatic turnover of colorimetric or
73 chemiluminescent substrates amplifies the signal (Gogalic et al. 2018).

74 The principles of ELISA have been adapted using advances in the protein array field to
75 increase the throughput, efficiency and scope of data in immunoassays (reviewed in Kingsmore
76 2006). Printing proteins can be carried out by passive adsorption without requiring modification
77 or chemical coupling to nanoparticles or other surfaces. This advantage and advancements in
78 nozzle technology allow for flexibility and precision in spotting picolitre volumes of purified,
79 crude, or complex proteinaceous substrates (Barbulovic-Nad et al. 2006). Furthermore, a
80 superior level of sensitivity can be achieved in miniaturized ligand-binding assays, as shown by
81 Ekins' ambient analyte assay theory (Ekins 1989). Obtaining higher sensitivity in a system that
82 uses smaller amounts of capture molecules and smaller amounts of sample can be explained by
83 two main features. First, the binding reaction occurs at a high target concentration; and second,
84 the capture-molecule–target complex is found only in the small area of the spot, resulting in a
85 high local signal (Templin et al. 2002). The most published format for protein array printing in
86 the infectious disease research setting is onto glass slides functionalized with nitrocellulose,
87 perhaps because both of the technical ease and that high density arrays are made possible by
88 printing onto this high protein binding flat surface (Davies et al. 2005; Desbien et al. 2013;
89 Koopmans et al. 2012; Nakajima et al. 2018; Price et al. 2013; te Beest et al. 2014). An
90 alternative format amenable for use in research labs is an ELISA-based microarray printed
91 directly onto the bottom of a 96-well plate (Mendoza et al. 1999). This method has been
92 validated against single plex assays (Liew et al. 2007) and has been adopted for biomarker

93 discovery in research labs (W. Huang et al. 2018; Y. Huang and Zhu 2017) and commercial
94 assays (e.g. PBL Assay Science, Piscataway, NJ; Quantarix, Billerica, MA; BioVendor LLC,
95 Asheville, NC; RayBiotech Inc., Peachtree Corners, GA). However, to date the 96-well format
96 has been infrequently applied to infectious disease antigens (Kang et al. 2012; Wang et al. 2015),
97 warranting more published examples and methods of applied research in this area.

98 For our multiplexed infectious disease research, we decided to capitalize on the
99 resources, familiarity and knowledge readily available for the conventional 96-well plate ELISA
100 and adapt the workflow directly to an in-house 96-well plate ELISA-Array format. The only
101 changes in the assay format were at the first and final steps. Using Maxisorp™ 96-well plates in
102 the first step, in lieu of coating a single antigen per well, we printed 1 nanoliter volumes of 8
103 viral antigens, in triplicate, per well. In the final step, a precipitating form of TMB substrate and
104 an array plate reader were needed for the ELISA-Array instead of the soluble TMB form and
105 general lab plate reader. The remainder of the workflow and reagents were identical in both
106 formats. The development and testing of the ELISA-Array was carried out using healthy human
107 donor plasma sampled post-vaccination (from the 2018 FluLaval vaccine), and assayed on
108 printed vaccine, recombinant hemagglutinin trimers, and purified FluB virus. Here we provide
109 data characterizing the ELISA-Array methods, advantages, precision, robustness, sensitivity,
110 stability and utility in infectious disease research.

111 **RESULTS**

112 **Initial optimization of printing conditions**

113 Although many operating conditions for printing followed the standard recommendations of the
114 manufacturer of the sciFLEXARRAYER S12 instrument, several specific parameters were
115 optimized for this ELISA-Array application. We tested variations in printing protein
116 concentration, drop volume and formulation buffer using goat anti-human Fc polyclonal
117 antibody (Jackson ImmunoResearch, West Grove, PA) as a probe with commercially available
118 human reference serum (Bethyl Laboratories, Montgomery, TX) as an analyte. The probe was
119 varied by diluting a PBS stock in a 1:1 volume of each of three sciSPOT protein formulation
120 buffers D1, D11 and D12 (Scienion AG, Berlin, Germany). Probe was dispensed in 1, 2 or 4
121 drops from a 384-well source plate at 25, 100 and 400 ug/mL final. PBS in formulation buffers
122 without the anti-human Fc protein was used for a background control. The probes of the printed

123 arrays bound to the Fc region of IgG within the human plasma, then are detected with HRP
124 conjugate antibodies specific to the kappa light chain of the IgG antibody in a traditional
125 sandwich ELISA format.

126 The signal intensity increased with increasing protein printed, and 400 ug/mL provided
127 the highest signal. The spot size increased with drop number, but the sensitivity was similar
128 between 2 and 4 drops. The protein stabilizing D12 buffer offered the highest sensitivity among
129 formulation buffers to approximately 4 ng/ml concentrations of IgG detected from human sera.
130 These data are shown in Supplementary Figure S1. The final printing parameters used in this
131 report for Influenza antigens are described in the methods section. Twelve 96-well plates were
132 printed in one batch with the Influenza antigens listed in Table 1 and using the array pattern
133 illustrated in Figure 1.

134

135 **Assay miniaturization gain of sensitivity in ELISA-Array**

136 According to the ambient assay theory (Ekins 1989), miniaturizing the ELISA to an array print
137 of 0.25ng of protein in a 200um spot (with a surface area of 15.6mm², or 0.02ng/mm²) should
138 yield higher sensitivity than coating in the same proportion over an entire 96-well (with a surface
139 area of 320mm²). We tested this by comparing the signal sensitivity obtained using human
140 immune reference plasma binding purified H1N1 HA trimer, either printed in 0.25ng spots in
141 triplicate or coated in a 96-well at 1000, 100, 10 or 1 ng in duplicate. Following the same assay
142 methods with the exception of the final TMB substrate (soluble for the ELISA and precipitating
143 for the ELISA-Array), equivalent IC₅₀ values were obtained only when the 96-well was coated
144 with 2000-fold more total protein, or >150-fold more/mm² (Figure 2).

145

146 **Data analysis**

147 After calculating median intensity in absorbance units (AU) of each triplicate set of antigen
148 spots, we fit standard 4-parameter logistic (4P) curves of intensity against plasma or mAb
149 concentration with PRISM (GraphPad, San Diego, CA). In each plate we tested three negative
150 controls to calculate the lower limit of detection, and on average the LOD value was less than 5
151 AU. Because the variance in readings at values less than 10 AU was high (data not shown), we
152 set a lower limit of detection (LLOQ) at 10 AU. From the 4P curves fit to each sample we
153 calculated both the titer at which the curve passed the LLOQ and the IC₅₀ values. Across our

154 assays we observed that the upper intensity range was never greater than 180 AU and thus set
155 limits of 0-200 AU in 4P curve fitting. Because at high concentrations the hook effect can lead to
156 reduced intensity readings (Tighe et al. 2015), we disregard any decreased values at high analyte
157 concentrations.

158

159 **ELISA-Array Sensitivity and Specificity**

160 In each ELISA-Array assay, polyclonal human immune reference plasma and monoclonal
161 antibodies of known binding activity were used to control for assay performance and determine
162 sensitivity. The dose-dependent binding of each of these controls over three independent assays
163 (Figure 3), IC₅₀ values and LLOQ are reported in Table 2. mAb A is known to be a neutralizing
164 antibody recognizing a conformationally dependent epitope on the stalk region of HA trimers
165 (Kallewaard et al. 2016) and was detected against the array of Influenza antigens from 10-
166 120ng/mL, well below the quantitative ug/mL range of relevant protective antibody levels *in vivo*
167 (Crum-Cianflone et al. 2012; Semenova et al. 2004). Reference plasma showed Influenza
168 antigen binding IC₅₀ values of 1.4×10^5 to 9×10^6 and titers of 6.4×10^4 to 1×10^6 (Figure 3 and
169 Table 2). These values reflect a polyclonal mixture of antibodies of any isotype since detection
170 was not limited to IgG (a cocktail of anti-kappa and anti-lambda light chain secondary antibodies
171 was used). The correlation of binding titers to protection varies by disease and for Influenza has
172 not been shown to be predictive (Madore et al. 2010). However, since binding is a pre-requisite
173 for neutralization activity, plasma titer can demonstrate the variation, breadth and magnitude of
174 viral antigen specificity between individuals.

175 The specificity of the assay was tested by measuring cross-reactivity at 200nM
176 concentrations of two irrelevant mAbs to any of the printed proteins: one directed to the
177 envelope protein of Dengue virus and the other to the RSV fusion protein. No signal was
178 observed in the assay with these mAbs. Specificity was also tested by printing a GFP-foldon-
179 Avitag-6His trimer in each well as a negative control protein, at the same concentration as the
180 Influenza A HA trimers. This control showed no binding to donor plasma or to control antibodies
181 mAb A and mAb B.

182 The lack of binding of control mAb A to the HA trimer of A/Shanghai/02/2013 H7N9
183 was not expected based on publications of this mAb binding to other H7 strains of HA, albeit at
184 lower affinities than other HA subtypes (Kallewaard et al. 2016). Reference plasma and other

185 donor plasma did bind the H7 trimer (Figures 3 and 4). A repeat test print of the H7 HA trimer at
186 0.5, 0.375 and 0.25ng/spot did not change the binding results, nor did testing on a regular ELISA
187 format (data not shown). Further optimization of this antigen, and comparisons to other strains
188 are needed in order to draw conclusions on cross-reactive antibody binding to H7.

189

190 **ELISA-Array assay performance**

191 The ELISA-Array assay was qualified using a selected in-house human reference plasma and
192 eight individual human plasma samples from day 28 post-vaccination with the 2018 FluLaval
193 quadrivalent vaccine (GlaxoSmithKline, Research Triangle Park, NC). All array plates used for
194 performance testing were from one print batch, stored at 4°C. To increase accuracy, we avoided
195 making large dilutions by preparing stock solutions of 10x reference plasma, 10x control mAbs,
196 100x secondary biotinylated antibody mixture, and 100x streptavidin conjugate in assay diluent.
197 These were aliquoted and stored at -80°C. Each plasma donor was also aliquoted undiluted and
198 stored at -80°C. Although not done in these assays, it would be optimal in the future to briefly
199 spin down donor plasma before assaying to clear the sample of lipid and other aggregates.
200 Aliquots were freshly thawed for each assay, and the same lot of assay diluent and TMB
201 substrate were also used throughout all assays. The final concentrations of assay materials are
202 described in the methods section. Intra-assay precision was determined by running n=3 plate
203 assays on the first day after printing the arrays. Inter-assay precision was determined by running
204 an additional two plates one and two weeks later. Precision was calculated by the variance
205 between plates of titer and IC₅₀ values for reference plasma and each of the eight donors for all
206 array antigens. Intra- and Inter-assay precision data is shown for the reference plasma and two
207 donors in Figure 4, and Tables 3 and 4, respectively, and for all eight plasma samples in
208 Supplementary Tables S1 and S2. The precision of absorbance units among the reference plasma
209 and two donors showed mean CV of 4.8% intra-assay and 10.8% inter-assay, and 6.0% intra-
210 assay and 12.5% inter-assay among the eight donor samples. There were a few examples of high
211 variance inter-assay, in samples of low dilutions. This may be due to weak binding or
212 interference from the serum matrix. The plasma titers could be differentiated by donor and
213 antigen with sensitivities ranging from 1 x 10³ to 4 x 10⁶ and IC₅₀ values from 1 x 10⁴ to 9 x 10⁶
214 (Figure 4, Table 4, and Table S2). For example, we measured a robust titer in the reference
215 plasma donor to all array antigens (Figure 4). In contrast, robust titers in donor 1 plasma were

216 measured only to the vaccine itself, to Influenza B viruses and to the individual antigens of
217 H1N1 and H3N2 HA trimers matching the strains used in the vaccine (Table 1 and Figure 4).
218 There was only weak binding to HA trimers not in the vaccine (i.e. H2, H5, H7), indicating
219 insufficient cross-reactive antibodies were elicited in donor 1. A plot of IC₅₀ values in Figure 5
220 for three donors shows the overall tight standard deviations between three assays performed over
221 three weeks, and visually quantifies differences between antibody binding for each of the array
222 antigens and donors. We cannot differentiate pre-existing antibody immunity from vaccine
223 responses in these samples, but the quantitative nature of the data would allow for this to be done
224 using titer and IC₅₀ comparisons with pre-vaccine plasma, not included in this study. Three
225 rounds of freeze thaws of the reference plasma from -80°C showed no change in IC₅₀ values or
226 titers (data not shown). One plate assay was also run by a second operator to evaluate the
227 robustness of the method, which was determined to be equivalent to intra-assay precision (Plate
228 4 in Figure 6 and Table S3).

229

230 **Stability testing of printed plates**

231 Printed array plates were covered with a foil plate seal and vacuum-sealed immediately after the
232 overnight curing step and stored at 4°C. They were found to be stable stored in this manner for
233 up to one month (Figure 6). At 8 weeks post-print, plates stored at 4°C showed about a 2-fold
234 drop in IC₅₀ and the titer shifted to one higher dilution in the ¼ titration series (i.e. a change from
235 1×10^6 to 2.6×10^5). Significant losses in activity were also measured for vacuum-sealed plates
236 stored for 1 week at either ambient temperature or 37 °C (Figure 6). All of the stability assay data
237 including variability for each antigen and plasma sample are provided in Supplementary Tables
238 S4 and S5. Using a different print lot, we tested the plates for 2-days at ambient temperature and
239 found them to be stable (data not shown).

240

241 **TABLES**

242 Table 1. Antigens included in the protein microarrays.

Influenza Strain	Subtype
A/Michigan/45/2015*	H1N1
A/Japan/305+/1957	H2N2
A/Singapore/INFIMH-16-0019/2016*	H3N2
A/Viet Nam/1194/2004	H5N1
A/Shanghai/02/2013	H7N9
B/Phuket/3073/2013-like virus* (B/Yamagata/16/88 lineage)	Influenza B
B/Colorado/06/2017-like virus* (B/Victoria/2/87 lineage)	Influenza B
Flulaval Vaccine 2018-2019	*H1N1, *H3N2, *Influenza B -1, *Influenza B -2

243 * components of the WHO recommended seasonal flu vaccine for 2018-19

244

245 Table 2. Sensitivity of reference mAbs and reference plasma pAb on ELISA-array antigens.

Antigen	IC₅₀ (ng/mL)	LLOQ (ng/mL)	Plasma titer IC₅₀	Plasma titer LLOQ
mAb A			Reference plasma	
Vaccine	1900	470	1.4e5	2.6e5
H1N1	110	10	8.5e6	1.0e6
H2N2	380	120	1.3e5	2.6e5
H3N2	170	30	4.0e5	2.6e5
H5N1	40	10	3.0e5	2.6e5
H7N9	>30,000	>30,000	2.9e5	6.4e4
mAb B				
Vaccine	7.3	2		
Influenza B1	238	125	9.0e6	1.0e6
Influenza B2	25	2	4.6e6	1.0e6

246

247

248 Table 3. Intra-assay precision from three donor plasma samples on ELISA-array antigens.^{1,2,3}

	Reference				Donor 1				Donor 6			
	1	2	3	%CV	1	2	3	%CV	1	2	3	%CV
Flulaval seasonal vaccine 2018-2019												
1e3	99.5	114.4	118.6	9.1	133.0	136.6	135.8	1.4	150.4	144.4	146.3	2.1
4e3	152.5	146.5	144.6	2.8	100.6	104.6	112.7	5.8	114.4	108.7	101.9	5.8
1.6e4	135.4	137.2	132.9	1.6	106.3	108.7	100.6	3.9	58.1	52.7	49.8	7.9
6.4e4	89.0	87.7	90.0	1.3	53.4	53.5	49.5	4.4	17.7	14.4	15.5	10.7
2.6e5	36.4	36.8	32.8	6.3	15.5	15.1	14.1	4.8	3.5	2.6	2.6	OOOR
1e6	9.9	9.6	9.6	OOOR	4.2	4.4	3.0	OOOR	2.2	0.4	0.2	OOOR
4.1e6	1.6	0.0	1.9	OOOR	0.5	0.2	1.1	OOOR	0.0	0.1	0.2	OOOR
1.6e7	0.4	0.4	1.0	OOOR	0.1	0.1	0.2	OOOR	0.5	0.0	0.0	OOOR
H1N1 HA trimer A/Michigan/45/2015												
1e3	100.2	103.7	118.4	9.0	149.3	145.3	153.3	2.7	138.7	149.6	140.3	4.1
4e3	148.0	142.6	150.9	2.9	154.7	153.5	158.8	1.8	125.9	123.5	121.0	2.0
1.6e4	143.5	132.3	139.4	4.1	118.1	119.7	119.2	0.7	70.7	67.9	67.5	2.5
6.4e4	100.1	101.1	103.7	1.8	58.5	61.8	62.4	3.5	21.4	21.0	22.6	3.8
2.6e5	45.3	48.4	43.8	5.1	15.8	16.8	18.2	7.2	4.7	5.4	5.7	OOOR
1e6	11.9	13.2	13.5	6.6	3.1	4.1	3.2	OOOR	0.8	0.0	0.7	OOOR
4.1e6	3.1	0.9	3.5	OOOR	0.0	1.0	0.0	OOOR	0.3	0.1	0.2	OOOR
1.6e7	0.1	0.1	1.2	OOOR	0.0	0.1	0.2	OOOR	0.2	0.0	0.0	OOOR
H2N2 HA trimer A/Japan/305+/1957												
1e3	109.6	129.4	141.9	12.9	58.7	65.8	66.8	6.9	113.0	118.6	101.3	7.9
4e3	115.1	145.6	137.9	11.9	24.7	25.4	26.1	2.8	88.3	99.7	96.8	6.2
1.6e4	111.8	111.7	104.4	3.9	5.9	5.6	5.8	OOOR	46.1	50.6	49.3	4.8
6.4e4	80.9	80.0	80.9	0.7	1.1	0.7	0.8	OOOR	12.7	12.8	14.3	6.8
2.6e5	28.5	32.7	30.5	6.9	0.1	0.4	0.2	OOOR	2.5	2.7	0.5	OOOR
1e6	7.6	8.0	8.6	OOOR	0.1	0.1	0.0	OOOR	0.6	0.1	0.3	OOOR
4.1e6	0.8	2.0	0.0	OOOR	0.1	0.0	0.0	OOOR	0.2	0.0	0.1	OOOR
1.6e7	0.2	0.1	0.8	OOOR	0.1	0.1	0.0	OOOR	0.1	0.0	0.0	OOOR
H3N2 trimer A/Singapore/INFIMH-16-0019/2016												
1e3	103.0	114.5	111.2	5.4	147.4	157.5	158.8	4.1	104.9	114.4	107.8	4.5
4e3	127.6	124.7	132.6	3.1	122.5	128.0	125.9	2.2	61.4	61.3	62.4	1.0
1.6e4	89.5	89.1	88.9	0.3	66.4	68.8	68.1	1.9	18.0	21.0	22.7	11.5
6.4e4	43.2	45.4	45.0	2.6	20.6	22.2	21.0	3.9	4.9	4.8	5.7	OOOR
2.6e5	12.7	12.4	11.7	3.9	5.8	5.1	5.3	OOOR	0.4	0.8	0.5	OOOR
1.0e6	3.2	3.1	2.4	OOOR	0.5	0.7	0.5	OOOR	0.5	0.0	0.2	OOOR
4.1e6	0.5	0.0	1.2	OOOR	0.4	0.3	0.7	OOOR	0.1	0.3	0.4	OOOR
1.6e7	0.2	0.1	0.9	OOOR	0.1	0.0	0.2	OOOR	0.0	0.0	0.0	OOOR
H5N1 A/Viet Nam/1194/2004												
1e3	130.6	120.0	124.8	4.2	43.6	61.7	72.9	24.9	115.3	120.5	113.7	3.0
4e3	112.7	129.5	130.9	8.1	25.3	33.1	29.7	13.4	71.7	71.7	73.3	1.3
1.6e4	71.3	82.7	88.2	10.7	6.3	8.6	8.8	OOOR	26.0	26.7	28.2	4.2
6.4e4	49.2	54.5	52.1	5.0	0.5	2.2	1.1	OOOR	5.4	6.4	6.1	OOOR
2.6e5	14.3	14.5	13.7	3.0	0.2	0.2	0.7	OOOR	0.4	0.9	0.3	OOOR
1.0e6	2.8	3.1	2.9	OOOR	0.4	0.1	0.0	OOOR	1.0	0.1	0.2	OOOR
4.1e6	0.3	0.0	0.8	OOOR	0.2	0.0	0.6	OOOR	0.1	0.1	0.2	OOOR
1.6e7	0.0	0.0	1.1	OOOR	0.0	0.0	0.0	OOOR	0.1	0.0	0.0	OOOR

	Reference				Donor 1				Donor 6			
	1	2	3	%CV	1	2	3	%CV	1	2	3	%CV
H7N1 HA trimer A/Shanghai/02/2013												
1e3	81.6	69.0	80.9	9.2	23.5	27.5	17.3	22.5	78.4	102.1	94.6	13.2
4e3	96.7	95.5	104.1	4.7	0.3	2.8	4.7	0.0	42.7	51.1	50.3	9.7
1.6e4	81.4	73.7	78.4	5.0	0.0	0.5	3.4	0.0	16.5	16.3	15.7	2.7
6.4e4	35.8	37.1	36.7	1.9	0.2	0.2	0.0	0.0	3.6	2.8	3.8	0.0
2.6e5	10.3	7.7	9.5	0.0	0.1	0.0	0.4	0.0	0.2	0.5	0.8	0.0
1.0e6	2.2	2.0	2.0	0.0	0.0	0.0	0.0	0.0	0.3	0.1	0.1	0.0
4.1e6	0.7	0.0	0.8	0.0	0.1	0.2	0.3	0.0	0.1	0.0	0.1	0.0
Influenza B/Phuket/3073/2013-like virus (B/Yamagata/16/88 lineage)												
1e3	71.9	118.8	129.4	28.7	154.7	159.6	158.8	1.7	109.4	139.5	138.5	13.3
4e3	38.5	96.1	105.4	45.3	160.4	162.7	165.6	1.6	145.0	144.3	150.9	2.5
1.6e4	152.0	160.6	146.6	4.6	142.7	148.3	147.4	2.0	108.5	112.7	111.0	1.9
6.4e4	130.1	150.9	151.3	8.4	86.2	86.9	84.5	1.4	50.3	54.8	56.6	6.0
2.6e5	87.6	90.9	86.4	2.7	31.7	30.9	35.0	6.6	15.1	15.0	15.3	1.0
1.0e6	33.4	33.9	33.8	0.8	6.9	8.1	7.9	0.0	3.1	2.8	4.7	0.0
4.1e6	7.8	10.0	10.0	13.6	1.2	1.7	2.1	0.0	0.2	0.9	0.4	0.0
Influenza B/Colorado/06/2017-like virus (B/Victoria/2/87 lineage)												
1e3	112.9	98.2	152.2	23.1	166.6	168.4	170.1	1.0	117.7	132.9	143.1	9.7
4e3	118.8	123.7	145.9	11.1	167.9	163.1	161.7	2.0	150.1	152.8	151.4	0.9
1.6e4	150.4	165.4	158.3	4.8	125.1	123.2	119.6	2.3	99.0	100.2	100.8	0.9
6.4e4	136.6	138.0	138.7	0.8	62.0	63.1	59.4	3.1	40.9	41.4	42.8	2.4
2.6e5	72.9	72.7	68.4	3.5	19.8	21.6	21.9	5.4	10.6	10.0	11.1	5.0
1.0e6	25.0	26.1	24.4	3.4	4.7	6.2	5.5	0.0	3.0	1.8	2.9	0.0
4.1e6	6.5	6.5	8.2	0.0	1.0	0.4	1.7	0.0	0.4	0.5	0.1	0.0

249 ¹Hook effect on low dilution points of titrations and all CV values are shown in grey.

250 ²0.0 indicates values below the lower level of quantitation signal of 10 (LLOQ).

251 ³Values in bold are the titers where signal is greater or equal than the LLOQ of 10.

252

253

254 Table 4. Inter-assay precision from three donor plasma samples on ELISA-array antigens.^{1,2,3}

	Reference				Donor 1				Donor 6			
	1	2	3	%CV	1	2	3	%CV	1	2	3	%CV
Flulaval seasonal vaccine 2018-2019												
1e3	105.2	97.3	99.4	4.1	138.3	110.5	132.3	11.5	148.4	138.3	142.4	3.6
4e3	146.8	150.0	102.8	19.8	108.7	110.7	106.6	1.9	116.2	95.9	128.4	14.5
1.6e4	128.4	109.1	120.0	8.1	97.2	112.4	89.8	11.6	133.0	138.7	134.7	2.1
6.4e4	77.5	84.2	75.8	5.6	46.1	60.5	40.3	21.3	105.6	94.9	92.3	7.2
2.6e5	31.3	29.1	32.0	5.1	13.1	15.6	11.1	17.0	51.4	41.9	42.2	11.9
1e6	7.4	9.1	8.0	OOOR	4.3	5.5	3.2	OOOR	15.3	12.5	10.9	17.1
4.1e6	1.0	1.1	0.6	OOOR	0.5	0.4	0.4	OOOR	3.0	3.5	3.9	OOOR
1.6e7	0.1	0.4	0.2	OOOR	0.0	0.4	0.5	OOOR	0.6	0.7	0.4	OOOR
H1N1 HA trimer A/Michigan/45/2015												
1e3	124.5	119.8	102.6	10.0	155.7	131.1	143.3	8.6	132.8	144.2	129.0	5.9
4e3	156.2	139.4	136.6	7.3	153.9	151.9	143.0	3.9	121.2	129.2	107.6	9.2
1.6e4	141.6	129.7	137.5	4.5	114.2	119.0	106.8	5.5	71.8	74.1	57.6	13.2
6.4e4	97.3	95.3	98.4	1.6	58.1	64.5	52.4	10.4	25.6	28.8	18.7	21.1
2.6e5	46.4	42.4	49.2	7.5	17.4	18.7	14.2	14.0	5.2	6.4	4.2	OOOR
1e6	11.5	11.3	12.3	4.6	4.2	5.1	3.0	OOOR	0.2	0.8	0.6	OOOR
4.1e6	1.7	2.5	3.9	OOOR	0.0	0.0	0.1	OOOR	0.1	0.0	0.2	OOOR
1.6e7	0.4	0.3	0.2	OOOR	0.6	0.2	0.0	OOOR	0.0	0.1	0.0	OOOR
H2N2 HA trimer A/Japan/305+/1957												
1e3	110.7	123.7	80.5	21.1	67.4	41.8	57.1	23.2	107.8	122.4	99.5	10.5
4e3	142.3	116.1	104.6	16.0	24.7	28.5	25.9	7.3	83.0	91.6	98.6	8.6
1.6e4	120.8	96.6	127.5	14.1	5.2	6.9	5.7	OOOR	53.8	54.1	45.7	9.3
6.4e4	78.9	73.8	85.1	7.1	1.1	0.6	0.7	OOOR	17.3	19.7	12.7	21.6
2.6e5	30.2	23.7	34.6	18.4	0.1	0.0	0.5	OOOR	2.3	3.6	2.0	OOOR
1e6	6.0	6.4	8.8	OOOR	0.3	0.0	0.3	OOOR	0.5	0.6	0.4	OOOR
4.1e6	0.8	0.2	1.8	OOOR	0.2	0.0	0.0	OOOR	0.1	0.2	0.1	OOOR
1.6e7	0.1	0.7	0.4	OOOR	0.2	0.1	0.4	OOOR	0.0	0.4	0.0	OOOR
H3N2 trimer A/Singapore/INFIMH-16-0019/2016												
1e3	97.8	115.4	108.1	8.2	157.4	136.2	150.3	7.3	112.1	100.1	85.1	13.7
4e3	140.2	114.0	119.5	11.1	128.6	133.8	119.6	5.6	63.4	69.3	54.3	12.1
1.6e4	95.3	71.9	88.5	14.1	65.7	76.6	61.9	11.2	22.9	23.2	16.0	19.7
6.4e4	42.1	35.2	39.2	8.9	19.8	25.4	19.6	15.2	5.7	5.2	4.2	OOOR
2.6e5	11.6	9.4	11.6	11.5	5.2	5.9	4.5	OOOR	1.3	0.9	0.3	OOOR
1.0e6	3.5	1.8	2.8	OOOR	4.9	0.7	0.3	OOOR	0.2	0.2	0.2	OOOR
4.1e6	0.5	0.9	0.3	OOOR	0.3	0.5	0.1	OOOR	0.3	0.2	0.2	OOOR
1.6e7	0.4	0.0	0.2	OOOR	0.5	0.2	0.2	OOOR	0.1	0.1	0.0	OOOR
H5N1 A/Viet Nam/1194/2004												
1e3	115.0	96.6	86.7	14.4	64.4	21.4	36.8	53.3	109.3	65.7	68.2	30.2
4e3	142.5	94.1	97.9	24.1	32.3	19.9	21.1	28.0	72.8	66.2	66.0	5.6
1.6e4	79.1	48.2	83.2	27.2	8.8	5.8	6.2	OOOR	27.7	30.4	23.0	13.7
6.4e4	49.0	42.7	53.0	10.8	1.3	0.7	1.1	OOOR	7.2	7.0	4.9	OOOR
2.6e5	14.7	12.0	16.2	14.8	0.2	0.2	0.1	OOOR	1.1	1.1	0.5	OOOR
1.0e6	2.7	3.3	3.5	OOOR	0.1	0.2	0.0	OOOR	0.2	0.2	0.2	OOOR
4.1e6	0.5	0.6	0.5	OOOR	0.1	0.0	0.1	OOOR	0.0	0.1	0.2	OOOR
1.6e7	0.4	0.2	0.1	OOOR	0.0	0.2	0.1	OOOR	0.0	0.0	0.1	OOOR

	Reference				Donor 1				Donor 6			
	1	2	3	%CV	1	2	3	%CV	1	2	3	%CV
H7N1 HA trimer A/Shanghai/02/2013												
1e3	95.1	115.2	98.9	10.3	24.9	8.8	21.2	11.5	92.8	83.6	85.7	5.5
4e3	113.7	84.2	97.7	15.0	1.5	6.1	5.7	OOOR	57.3	66.4	54.4	10.6
1.6e4	86.7	75.7	82.9	6.8	0.7	7.3	0.6	OOOR	19.2	23.1	17.7	14.0
6.4e4	34.9	33.6	42.9	2.7	0.2	0.1	0.0	OOOR	4.7	4.6	3.3	OOOR
2.6e5	9.9	9.9	13.0	OOOR	0.0	0.0	0.1	OOOR	3.0	2.2	3.0	OOOR
1.0e6	2.4	2.1	3.1	OOOR	0.2	0.3	0.3	OOOR	0.9	0.2	0.8	OOOR
4.1e6	0.3	0.3	0.5	OOOR	0.2	0.1	0.0	OOOR	0.1	0.3	0.1	OOOR
Influenza B/Phuket/3073/2013-like virus (B/Yamagata/16/88 lineage)												
1e3	111.6	86.4	101.8	12.7	140.5	130.5	153.5	8.2	138.1	91.6	104.7	21.5
4e3	103.1	127.5	94.7	15.7	157.7	158.3	158.2	0.2	152.9	144.4	141.4	4.1
1.6e4	150.0	153.2	145.7	2.5	142.6	148.5	142.6	2.4	116.6	123.5	107.7	6.8
6.4e4	142.4	135.6	146.5	3.9	84.2	90.8	81.9	5.4	61.4	63.2	51.2	11.1
2.6e5	87.5	86.5	94.1	4.6	30.7	35.1	28.8	10.3	17.2	19.9	12.8	21.5
1.0e6	33.5	35.4	38.8	7.6	7.3	8.9	6.4	OOOR	4.1	5.4	3.7	OOOR
4.1e6	9.6	8.1	9.9	OOOR	0.6	0.9	1.3	OOOR	0.7	0.9	0.7	OOOR
Influenza B/Colorado/06/2017-like virus (B/Victoria/2/87 lineage)												
1e3	103.4	112.5	99.1	6.6	168.5	164.0	164.4	1.5	137.8	147.5	110.3	14.6
4e3	142.9	133.5	133.8	3.9	161.3	162.6	158.3	1.4	149.8	162.4	146.3	5.6
1.6e4	161.3	159.7	158.8	0.8	119.9	122.3	121.6	1.0	102.4	111.7	95.6	7.8
6.4e4	130.2	127.5	125.6	1.8	59.8	66.9	62.6	5.7	47.9	50.8	37.8	15.0
2.6e5	69.2	70.3	74.4	3.9	19.1	22.9	19.3	10.5	12.8	14.0	9.3	20.2
1.0e6	26.0	24.0	27.6	6.8	4.8	6.4	5.0	OOOR	3.0	3.8	2.5	OOOR
4.1e6	6.4	6.8	6.8	OOOR	0.2	0.6	0.9	OOOR	0.5	0.6	1.0	OOOR

255 ¹Hook effect on low dilution points of titrations and all CV values are shown in grey.

256 ²OOOR indicates values below the lower level of quantitation of 10.

257 ³Values in bold are the titers where signal is greater or equal than the LLOQ of 10.

258

259 Table 5. Intra-assay and Inter-assay precision of plasma IC₅₀ values on ELISA-Array antigens.

	Reference				Donor 1				Donor 6			
	1	2	3	%CV	1	2	3	%CV	1	2	3	%CV
Flulaval seasonal vaccine 2018-2019												
Intra	1.2e5	1.1e5	1.1e5	6.0	2.2e5	2.2e5	2.6e5	10.1	1.1e4	1.2e4	1.6e4	20.3
Inter	1.5e5	1.4e5	1.4e5	4.8	3.0e5	1.4e5	3.4e5	40.5	1.3e4	7.1e5	1.2e4	28.0
H1N1 HA trimer A/Michigan/45/2015												
Intra	8.6e6	7.3e6	8.6e6	8.8	2.24e5	2.0e5	2.2e5	6.3	6.4e5	8.1e5	7.1e5	11.8
Inter	1.0e5	8.4e6	7.1e6	17.6	2.6e5	2.4e5	2.6e5	4.1	5.6e5	6.2e5	8.1e5	20.0
H2N2 HA trimer A/Japan/305+/1957												
Intra	8.8e6	1.0e5	1.2e5	16.7	5.1e4	5.6e4	5.5e4	5.3	1.1e4	8.3e5	6.4e5	24.8
Inter	1.4e5	1.3e5	1.2e5	9.2	6.0e4	1.7e4	3.8e4	55.3	6.6e5	1.1e4	6.6e5	29.9
H3N2 trimer A/Singapore/INFIMH-16-0019/2016												
Intra	4.0e5	3.6e5	4.6e5	13.5	8.1e5	8.7e5	9.4e5	7.3	2.6e4	3.7e4	3.0e4	18.7
Inter	4.6e5	4.1e5	3.4e5	14.9	9.1e5	5.4e5	9.7e5	29.1	3.3e4	1.7e4	2.0e4	36.3
H5N1 A/Viet Nam/1194/2004												
Intra	5.2e5	5.2e5	4.2e5	12.0	2.4e4	3.0e4	7.6e4	66.0	2.3e4	2.7e4	2.0e4	14.4
Inter	5.6e5	1.9e5	1.4e5	75.8	3.6e4	9.3e5	2.6e4	56.2	1.9e4	9.8e5	7.9e5	48.4
H7N1 HA trimer A/Shanghai/02/2013												
Intra	2.4e5	2.6e5	3.0e5	13.0	>1e3	>1e3	>1e3	OOD	3.9e4	4.2e4	3.5e4	8.2
Inter	3.2e5	3.7e5	1.9e5	30.6	>1e3	>1e3	>1e3	OOD	2.3e4	1.2e4	2.1e4	31.6
Influenza B/Phuket/3073/2013-like virus (B/Yamagata/16/88 lineage)												
Intra	3.3e6	3.3e6	3.2e6	2.3	1.4e5	1.4e5	1.6e5	7.1	3.2e5	2.2e5	3.2e5	20.1
Inter	3.1e6	3.3e6	2.1e5	112.0	1.4e5	1.3e5	2.5e5	39.1	2.7e5	2.0e5	2.0e4	124.0
Influenza B/Colorado/06/2017-like virus (B/Victoria/2/87 lineage)												
Intra	4.2e6	5.2e6	4.5e6	11.4	2.6e5	2.7e5	3.0e5	7.7	2.3e5	2.8e5	3.2e5	15.7
Inter	4.5e6	5.7e6	3.8e6	21.3	2.9e5	2.3e5	2.5e5	10.0	2.7e5	3.8e5	5.1e5	30.6

260

261 DISCUSSION

262 An ability to print microarrays in a format for a 96-well ELISA-Array was first published by
 263 Mendoza et al. (1999), and its utility for infectious disease testing has been demonstrated with
 264 antibody arrays to encephalitis viruses (Kang et al. 2012) and viral antigen arrays to Flaviviridae
 265 (Wang et al. 2015), using a non-contact piezo Bio-Dot Printing System (Biodot, Irvine, CA). As
 266 with these two prior studies, we printed using non-contact piezo nozzles, but in smaller volumes
 267 using a Scienion S12 instrument. We compared binding data in arrays using a variety of
 268 Influenza antigen types including recombinant viral protein HA trimers, vaccine and viruses. The
 269 parallel identification of viral antigen binding was carried out in a quantitative manner by
 270 performing full dose-response curves of human plasma with an analysis of the precision of titer
 271 and IC₅₀ values. These data allowed for a comparison of the abundance and context of antibodies
 272 from natural exposure or vaccination within a single individual and between individuals. In

273 future arrays it would be of interest to include the Influenza neuramidase protein, a second viral
274 surface protein that can be targeted by neutralizing antibodies (Memoli et al. 2016). It is
275 important to note that the quality and relevance of protein array data is only as good as the
276 proteins printed. The use of reference monoclonal antibodies or plasma with known activity is
277 helpful to characterize the integrity of the protein reagents and printing conditions. Such
278 reference reagents can also serve to bridge data between different array print lots and stability as
279 well as between data from different operators or labs. Stability testing of the ELISA-Array plates
280 supports the ability to ship plates on cold packs to a collaborating research lab, with a tolerance
281 of up to 48 hours at ambient temperature. The collaborating lab would only incur the lesser cost
282 and training required for the array reader.

283 There is great potential to use what is learned from protein arrays in research labs
284 towards the design and testing of vaccines and for the development of simplified rapid point-of-
285 care testing (POCT) of infectious diseases. To date, POCT efforts have taken the form of printed
286 arrays on lateral flow test strips, a promising technology needing further development to be
287 useful in endemic, low resource settings (Kim, Chung, and Kang 2019; Urusov, Zherdev, and
288 Dzantiev 2019). Protein array data can also be a valuable tool for the identification of individuals
289 most likely to have acquired broadly cross-reactive and/or potent neutralizing antibodies to
290 infectious disease. Passive immunization with monoclonal antibodies can be highly effective in
291 controlling viral pathogenesis (Salazar et al. 2017), and an ability to screen the serum of human
292 donors suspected to be clinically protected from disease in a multiplexed and quantitative format
293 can help identify the best donor for antibody discovery. In this application it is valuable to have
294 functional neutralization assay data on the same sera, to correlate to binding.

295 Overall, we have provided new methods and qualification data to support applications
296 ELISA-Array assay format for infectious disease research. The key advantages we observed with
297 this technology included the passive coating in a protein stabilizing buffer, the low protein
298 reagent consumption with nanoliter printing, and the ability to perform quantitative analyses
299 using nearly the same workflow, reagents and lab equipment as used in the conventional ELISA.

300

301 **METHODS**

302 **Chemicals**

303 Phosphate buffered saline (Gibco DPBS, calcium and magnesium free, pH 7.2) and EDTA
304 (0.5M Ambion) were obtained from Thermofisher (Waltham, MA). PBS with 0.05%
305 Polysorbate-20 was purchased as a 20x stock from Teknova Inc. (Hollister, CA). Fraction V
306 bovine serum albumin (BSA), gamma-Globulins from bovine blood (BGG), ProClin 300 and
307 CHAPS were purchased from Sigma-Aldrich (St. Louis, MO). Fetal Bovine Serum (FBS), US
308 source, triple 0.1um filtered, was sourced from Omega Scientific (Tarzana, CA).

309

310 **General instrument and experimental parameters**

311 The Scienion sciFLEXARRAYER S12 instrument (Scienion AG, Berlin, Germany) has been
312 optimized for non-contact, piezo-acoustic dispensing of ultra-low volumes from an inert coated
313 glass capillary in a climate-controlled (temperature, dewpoint and humidity) environment, with
314 precise XYZ axis control and on-board camera and software for QC of each spot in the array.

315 We printed our arrays with the PDC70 type 3 nozzle (Scienion) due to its reduced
316 dispense volume and the specific hydrophobic coating optimized to improve the dispense
317 stability of protein solutions. The system liquid is Milli-Q Water filtered through the Milli-Q
318 Ultrapure Water System (Millipore Sigma, Burlington, MA) that is subsequently degassed for at
319 least 30 minutes in a sonicating water bath. Proteins were spotted on low dust, black, clear
320 bottom, high protein binding Fluotrac™ 600, Greiner Bio-One 96-well plates (Fisher Scientific,
321 Waltham, MA), positioned on a ceramic platform under vacuum. The printing was carried out at
322 60% humidity and ambient temperature, with drop volumes of 330-350 pL. The 384-well source
323 plate (Scienion) was kept at dewpoint. Drop stability and array quality were assessed for quality
324 for each run. Prior to dispensing into the plates, autodrop detection was used to assess drop
325 stability by quantifying the velocity, deviation and drop volume for each protein spotted. In
326 addition, all plates were imaged with the on-board head camera after the completion of spotting
327 to ensure correct alignment and spot diameters. Printed arrays were incubated overnight at 75%
328 relative humidity and ambient room temperature to allow adsorption of the proteins to the
329 binding surface of the plate. Plates were then vacuum packaged and stored at 4°C until ready for
330 use.

331 The sciREADER CL2 (Scienion) is used for the colorimetric reading of the final assay of arrays.
332 After images are taken of each well, the software analysis program aligns the spot pattern to the
333 imaged spots and calculates a median intensity in absorbance units (AU).

334 **Initial ELISA-Array assay used for optimization of parameters**

335 Initial 96-well printed arrays were printed according to the general instrument parameters
336 described above. All assay steps were performed at ambient temperature. Blocking solution
337 (sciBLOCK Protein DIM solution, Scienion) was added at 200 μ L/well with a multichannel
338 pipet and allowed to incubate without agitation for 1 hour. The block solution was manually
339 removed and the plate washed 1x by adding 300 μ L/well of sciWASH Protein D1 agitating at
340 350rpm for 5 minutes on a Bioshake iQ thermomixer. Dilutions of human reference serum (with
341 IgG quantified at 4.4 mg/ml; Bethyl Laboratories) were made in blocking buffer (PBS, 0.05%
342 Tween-20, and 0.5% BSA), and 100 μ L/well was added to the plate incubated for 1 hour with
343 gentle agitation (250 rpm). The arrays were manually washed 3 times with 2-5 min agitations in
344 between washes. A secondary polyclonal goat antibody (Southern Biotech, Birmingham, AL)
345 directed to the human kappa light chain and conjugated with horseradish peroxidase (HRP) was
346 used at 1/5000 in blocking buffer for 1 hour. After a second round of 3 manual washes the signal
347 was developed with sciCOLOR T2, a precipitating TMB reagent (Scienion), for 15 minutes.

348

349 **Influenza hemagglutinin proteins**

350 Recombinant hemagglutinin (HA) ectodomain constructs were made using gene blocks (IDT,
351 Newark, NJ) cloned into a pADD2 plasmid using EcoRI and XhoI restriction sites. The cloning
352 was performed with In-Fusion HD Cloning kit (Takara Bio, Mountain View, CA). Each
353 construct consisted of the native HA signal sequence, HA ectodomain, a trimeric foldon
354 domain of T4 fibronectin, an Avi tag sequence (GLNDIFEAQKIEWHE), and a hexa-histidine
355 affinity tag (Whittle J. et al., 2014). A negative control construct was made with the tags fused to
356 the GFP protein. Plasmids were purified with NucleoBond® Xtra Maxi kit (Macherey Nagel,
357 Düren, Germany) and transfected into Expi293 cells grown in a 1:2 mixture of Expi293 and
358 Freestyle (Gibco, Thermofisher Scientific) media. For transfection, 50 μ g of plasmid was pre-
359 incubated with 1.3 ml of FectoPRO transfection reagent (Polyplus, New York, USA) and added
360 to 1L of media. At day 4, the media was clarified by centrifugation (7500xg, 15 min), filtered,
361 and diluted 2-fold with PBS. The media was then batch incubated with HisPur Ni-NTA resin
362 (Thermofisher Scientific) for 2 hours at 4°C and loaded on a gravity flow column. The resin was
363 washed with 20 column volumes of PBS with 5 mM imidazole and eluted in 4 ml of PBS with
364 250 mM imidazole. The eluted protein was concentrated and loaded on a Superdex 200 16/60

365 column (GE Healthcare, Chicago, IL) pre-equilibrated with PBS. The elution fractions
366 corresponding to the trimeric HA proteins were pooled, concentrated, and stored in 10% glycerol
367 in PBS at -20°C.

368

369 **Human plasma and reference antibodies**

370 Post-vaccination (28 days) blood samples were collected from nine healthy volunteers who
371 received the 2018/2019 seasonal influenza vaccine (FluLaval quadrivalent vaccine,
372 GlaxoSmithKline, Research Triangle Park, NC) in the fall of 2018 following a protocol approved
373 by Stanford University (IRB protocol 48130). Plasma was separated from heparinized blood
374 samples by centrifugation at 500g for 15 minutes and stored at -20°C. One donor was identified
375 with the highest plasma titer to all Influenza antigens and was used as a reference in all assays.
376 Two specific positive control reference antibodies with characterized low nanomolar affinities to
377 HA trimers were cloned and made recombinantly as human IgG1 in Expi293 cells with methods
378 described previously (Durham et al. 2019): MEDI8852 for InfA group 1 and 2 HA (Kallewaard
379 et al), and TF19 for InfB HA (unpublished in-house reagent). Two recombinant mAbs were used
380 as cross-reactivity controls, J9 directed to the Dengue viral envelope (Durham et al. 2019) and
381 3D3 to the RSV fusion protein (Collarini et al. 2009).

382

383 **Printing of the Influenza protein array**

384 Protein stocks of recombinant proteins at 0.5 mg/mL in PBS or vaccine stocks were diluted 1:1
385 in D12 buffer, mixed by pipetting, transferred to a 384 well polypropylene plate
386 (sciSOURCEPLATE, Scienion), and centrifuged for 2 min at 1800xg ambient temperature to
387 eliminate debris or air bubbles. The pattern printed was a 6x6 spot array on each well, and each
388 protein or vaccine along with positive and negative controls was printed in triplicate, 3 spots per
389 well, with 3 drops printed per spot. A single lot of twelve 96-well plates were printed in one day,
390 and after overnight curing were either subject to the ELISA-Array assay the next day (plates 1-
391 4), subject to temperature variations for one week (plates 5-7), or subject to varying incubation
392 times at 4°C (plates 8-10).

393

394 **Influenza ELISA-Array assay**

395 Each 96-well printed array was printed according to the general instrument parameters described
396 above. All assay steps were performed at ambient temperature, incubations except the blocking
397 step were done with low agitation on a Titer Plate Shaker (Lab-line Instruments, Melrose, IL)
398 and washes were done using a BioTek ELx405 plate washer (Bio-Tek Instruments, Winooski,
399 VT). High agitation is avoided as it leads to comets around the spots, which interferes with
400 accurate spot definition during reading of absorbance intensity. Array plates were washed 1x 300
401 $\mu\text{L}/\text{well}$ before immediately adding 200 $\mu\text{L}/\text{well}$ of assay diluent (PBS, 0.5% BSA, 2% filtered
402 FBS, 0.2% BGG, 0.25% CHAPS, 5mM EDTA, 0.05% Polysorbate-20 and 0.05% ProClin 300,
403 pH 7.2) down the sides of the wells with a multichannel pipette. Plates were allowed to block for
404 1 hour. Human plasma was diluted 1/1000 in assay diluent and serially diluted $\frac{1}{4}$ for n=8 points.
405 After manual removal of blocking solution with a multichannel pipette, plasma titrations were
406 added with one donor per column of the plate and incubated for 2 hours. The arrays were washed
407 3x 300 $\mu\text{L}/\text{well}$ on the plate washer before adding 100 $\mu\text{L}/\text{well}$ of a 1/5000 cocktail of
408 biotinylated secondary polyclonal goat antibodies (Southern Biotech) directed to the human
409 kappa and lambda light chains in assay diluent. After 1 hour of incubation and 3x 300 $\mu\text{L}/\text{well}$
410 washing, a SA-HRP high sensitivity conjugate (Pierce) was added for 1 hour. After a final 3x
411 300 $\mu\text{L}/\text{well}$ wash, residual buffer was manually removed with a pipette and 50 $\mu\text{L}/\text{well}$ of
412 sciCOLOR T2 added for 20 minutes.

413

414 **Conventional ELISA**

415 The same high protein binding plates as used in the ELISA-Array were coated overnight at 4°C
416 with 100 $\mu\text{L}/\text{well}$ of the H1N1 A/Michigan/45/2015 strain of HA trimer in PBS, pH 7.2. The
417 ELISA assay was performed in the same manner as the ELISA-Array with the exception of the
418 development step. Plates were developed for 10 minutes with 50 $\mu\text{L}/\text{well}$ soluble TMB substrate
419 (KPL Sure Blue 1-component, SeraCare Life Sciences, Milford, MA) and stopped with 50
420 $\mu\text{L}/\text{well}$ of TMB Stop solution (KPL).

421

422

423 **FIGURE LEGENDS**

424

425 **Figure 1. The ELISA-Array print pattern.** The 6x6 array was printed in each well of a 96-well
426 plate. The outer edges contain fiducial spots of biotinylated anti-kappa antibody for orientation
427 (#11). All other spots are printed in triplicate, using anti-IgG Fc antibody as a positive control
428 (#1) and GFP-foldon as a negative control (#10). In the top half of the pattern are Influenza A
429 HA group I proteins (#2-4) and the 2018 vaccine (#5), and in the bottom half are Influenza A HA
430 group II proteins (#6-7) and Influenza B HA proteins (#8-9). At right is an image of one array
431 well developed after binding reference plasma on H1N1 A/Michigan/45/2015 HA trimer.
432

433 **Figure 2. A comparison of the amount of protein needed in ELISA versus ELISA-Array.**
434 Two sets of data are shown from a titration of a reference plasma on the H1N1
435 A/Michigan/45/2015 HA trimer. On the left, a conventional ELISA is shown using 4 different
436 antigen coat amounts. On the right, ELISA-array data is shown for the same antigen printed at
437 0.25ng where an equivalent IC_{50} is obtained when compared to the highest (1ug) antigen coat on
438 the conventional ELISA. The dashed line in ELISA-array plot indicates the lower limit of
439 quantification (10 AU).
440

441 **Figure 3. The sensitivity of the ELISA-Array.** Three sets of data are shown with the titration
442 of two monoclonal anti-Influenza antibodies and a reference plasma on the Influenza array
443 antigens. Panels show titrations of an anti-Influenza A mAb (left), an anti-Influenza B mAb
444 (center) and a reference plasma (right) against the array of Influenza A antigens (left & right),
445 Influenza B antigens (center & right), and the FluLaval 2018-2019 vaccine (all). Data is from 3
446 inter-assay plates, with mean and SD shown.
447

448 **Figure 4. Dose-response curves of 3 donors on the Influenza antigen array.** The dose-
449 dependent binding curves of a reference plasma (red), donor 1 plasma (blue) and donor 6 plasma
450 (green) to the Influenza antigen array are shown. The top left panel shows plasma titrations
451 against Influenza A group I HA trimers, the top right panel shows titrations against Influenza A
452 group II HA trimers, the bottom left panel shows titrations against Influenza B viruses, and the
453 bottom right panel shows titrations against the FluLaval 2018-2019 vaccine. Data is from 3 inter-
454 assay plates, with mean and SD shown.
455

456 **Figure 5. IC_{50} comparisons of 3 donors on the Influenza antigen array.** IC_{50} values
457 determined from 4-parameter fits of array antigen binding curves using a reference plasma (red),
458 donor 1 plasma (blue) and donor 6 plasma (green) are plotted. The top left panel shows IC_{50}
459 values against Influenza A group I HA trimers, the top right panel shows IC_{50} values against
460 Influenza A group II HA trimers, the bottom left panel shows IC_{50} values against Influenza B
461 viruses, and the bottom right panel shows IC_{50} values against the FluLaval 2018-2019 vaccine.
462 Data is from 3 inter-assay plates, with mean and SD shown. The IC_{50} value for donor 1 plasma
463 against H7 is not shown because the titer was greater than the minimum 1/1000 dilution.
464

465 **Figure 6. Intra-assay, Inter-assay and Stability Performance of the ELISA-Array.** Three
466 dose-dependent binding curves are shown using a reference plasma and the H1N1
467 A/Michigan/45/2015 HA trimer. The left panel shows both intra-assay error (plates #1-3) as well
468 as inter-operator robustness (plates #1-3 vs. #4). The center panel shows inter-assay error with
469 plates tested after increasing time periods stored at 4 °C. The right panel shows stability after 1
470 week at ambient temperature, at 37 °C and up to 8 weeks at 4 °C.

471

472 **SUPPLEMENTARY MATERIAL**

473 **Supplementary Figure S1. Optimization of printing parameters.** Initial tests of signal
474 intensity using different Scienion formulation buffers (D01 vs. D11 vs. D12), protein stock
475 concentrations (25 vs 100 vs 400 µg/mL), and number of drops (1 vs. 2 vs. 3). All spots are of
476 goat anti-human Fc, made in triplicate, and detected using anti-kappa HRP. BLK indicates buffer
477 background controls printed in the same array. Values in signal intensity are of human reference
478 serum dilutions from dark to light green of 1/1,000, 1/5,000, 1/10,000, 1/100,000, and
479 1/1,000,000.

480

481 **Supplementary Table S1.** Intra-assay precision (n=3 plates) from all eight donor plasma
482 samples, reference plasma, and 2 anti-Influenza mAbs on ELISA-array antigens.

483

484 **Supplementary Table S2.** Inter-assay precision (n=3 plates) from all eight donor plasma
485 samples, reference plasma, and 2 anti-Influenza mAbs on ELISA-array antigens.

486

487 **Supplementary Table S3.** Inter-operator robustness (n=2 plates) from all eight donor plasma
488 samples, reference plasma, and 2 anti-Influenza mAbs on ELISA-array antigens.

489

490 **Supplementary Table S4.** Stability of ELISA-Array plates at varying temperatures for 1 week
491 (n=3 plates) from all eight donor plasma samples, reference plasma, and 2 anti-Influenza mAbs
492 on ELISA-array antigens.

493

494 **Supplementary Table S5.** Stability of ELISA-Array plates under longer-term 4 °C storage (n=5
495 plates) from all eight donor plasma samples, reference plasma, and 2 anti-Influenza mAbs on
496 ELISA-array antigens.

497

498 **AUTHOR CONTRIBUTIONS**

499 KM and MS conceived and designed the study. EW, EC and KM carried out the experiments and
500 performed data analysis. NF produced the recombinant viral antigens. MS coordinated and
501 collected the donor plasma and provided the vaccine and virus materials. EW and KM wrote the
502 manuscript. All the authors read and approved the final manuscript.

503

504 **ACKNOWLEDGEMENTS**

505 The authors would like to thank Joshua Cantlon and Robert Kardish for their expert help with
506 establishing the initial parameters and training for ELISA-array printing.

507

508 **FUNDING**

509 This work was supported by the Chan Zuckerberg Biohub.

510

511 REFERENCES

- 512 Abbas, Abul K., Andrew H. Lichtman, and Shiv Pillai. 2014. *Cellular and Molecular*
513 *Immunology*. Philadelphia, PA: Elsevier Health Sciences.
- 514 Antia, Alice, Hasan Ahmed, Andreas Handel, Nichole E. Carlson, Ian J. Amanna, Rustom Antia,
515 and Mark Slifka. 2018. “Heterogeneity and Longevity of Antibody Memory to Viruses
516 and Vaccines.” *PLoS Biology* 16 (8): e2006601.
517 <https://doi.org/10.1371/journal.pbio.2006601>.
- 518 Barbulovic-Nad, Irena, Michael Lucente, Yu Sun, Mingjun Zhang, Aaron R. Wheeler, and
519 Markus Bussmann. 2006. “Bio-Microarray Fabrication Techniques—a Review.” *Critical*
520 *Reviews in Biotechnology* 26 (4): 237–59. <https://doi.org/10.1080/07388550600978358>.
- 521 Beest, Dennis te, Erwin de Bruin, Sandra Imholz, Jacco Wallinga, Peter Teunis, Marion
522 Koopmans, and Michiel van Boven. 2014. “Discrimination of Influenza Infection
523 (A/2009 H1N1) from Prior Exposure by Antibody Protein Microarray Analysis.” *PloS*
524 *One* 9 (11): e113021. <https://doi.org/10.1371/journal.pone.0113021>.
- 525 Collarini, Ellen J., F. Eun-Hyung Lee, Orit Foord, Minha Park, Gizette Sperinde, Hai Wu,
526 William D. Harriman, Stephen F. Carroll, Stote L. Ellsworth, and Larry J. Anderson.
527 2009. “Potent High-Affinity Antibodies for Treatment and Prophylaxis of Respiratory
528 Syncytial Virus Derived from B Cells of Infected Patients.” *The Journal of Immunology*
529 183 (10): 6338–45. <https://doi.org/10.4049/jimmunol.0901373>.
- 530 Crum □ Cianflone, N. F., G. Collins, G. Defang, E. Iverson, Lynn E. Eberly, C. Duplessis, J.
531 Maguire, A. Ganesan, B. K. Agan, and T. Lalani. 2012. “Immunoglobulin G Subclass
532 Levels and Antibody Responses to the 2009 Influenza A (H1N1) Monovalent Vaccine
533 among Human Immunodeficiency Virus (HIV) □ infected and HIV □ uninfected Adults.”
534 *Clinical & Experimental Immunology* 168 (1): 135–41. [https://doi.org/10.1111/j.1365-](https://doi.org/10.1111/j.1365-2249.2011.04550.x)
535 [2249.2011.04550.x](https://doi.org/10.1111/j.1365-2249.2011.04550.x).
- 536 Davies, D. Huw, Xiaowu Liang, Jenny E. Hernandez, Arlo Randall, Siddiqua Hirst, Yunxiang
537 Mu, Kimberly M. Romero, Toai T. Nguyen, Mina Kalantari-Dehaghi, and Shane Crotty.
538 2005. “Profiling the Humoral Immune Response to Infection by Using Proteome
539 Microarrays: High-Throughput Vaccine and Diagnostic Antigen Discovery.”
540 *Proceedings of the National Academy of Sciences* 102 (3): 547–52.
541 <https://doi.org/10.1073/pnas.0408782102>.
- 542 De Silva, Nilushi S., and Ulf Klein. 2015. “Dynamics of B Cells in Germinal Centres.” *Nature*
543 *Reviews Immunology* 15 (3): 137–48. <https://doi.org/10.1038/nri3804>.
- 544 Desbien, Anthony L., Neal Van Hoesen, Steven J. Reed, Allen C. Casey, John D. Laurance,
545 Susan L. Baldwin, Malcolm S. Duthie, Steven G. Reed, and Darrick Carter. 2013.
546 “Development of a High Density Hemagglutinin Protein Microarray to Determine the
547 Breadth of Influenza Antibody Responses.” *Biotechniques* 54 (6): 345–48.
548 <https://doi.org/10.2144/000114041>.
- 549 Durham, Natasha D., Aditi Agrawal, Eric Waltari, Derek Croote, Fabio Zanini, Mallorie Fouch,
550 Edgar Davidson, Olivia Smith, Esteban Carabajal, and John E. Pak. 2019. “Broadly
551 Neutralizing Human Antibodies against Dengue Virus Identified by Single B Cell
552 Transcriptomics.” *ELife* 8: e52384. <https://doi.org/10.7554/eLife.52384>.

- 553 Ekins, Roger P. 1989. "Multi-Analyte Immunoassay." *Journal of Pharmaceutical and*
554 *Biomedical Analysis* 7 (2): 155–68. [https://doi.org/10.1016/0731-7085\(89\)80079-2](https://doi.org/10.1016/0731-7085(89)80079-2).
- 555 Engvall, Eva, and Peter Perlmann. 1972. "Enzyme-Linked Immunosorbent Assay, ELISA: III.
556 Quantitation of Specific Antibodies by Enzyme-Labeled Anti-Immunoglobulin in
557 Antigen-Coated Tubes." *The Journal of Immunology* 109 (1): 129–35.
- 558 Gogalic, Selma, Ursula Sauer, Sara Doppler, and Claudia Preininger. 2018. "Investigating
559 Colorimetric Protein Array Assay Schemes for Detection of Recurrence of Bladder
560 Cancer." *Biosensors* 8 (1): 10. <https://doi.org/10.3390/bios8010010>.
- 561 Huang, Wei, Kelly Whittaker, Huihua Zhang, Jian Wu, Si-Wei Zhu, and Ruo-Pan Huang. 2018.
562 "Integration of Antibody Array Technology into Drug Discovery and Development."
563 *Assay and Drug Development Technologies* 16 (2): 74–95.
564 <https://doi.org/10.1089/adt.2017.808>.
- 565 Huang, Yi, and Heng Zhu. 2017. "Protein Array-Based Approaches for Biomarker Discovery in
566 Cancer." *Genomics, Proteomics & Bioinformatics* 15 (2): 73–81.
567 <https://doi.org/10.1016/j.gpb.2017.03.001>.
- 568 Kallewaard, Nicole L., Davide Corti, Patrick J. Collins, Ursula Neu, Josephine M. McAuliffe,
569 Ebony Benjamin, Leslie Wachter-Rosati, Frances J. Palmer-Hill, Andy Q. Yuan, and
570 Philip A. Walker. 2016. "Structure and Function Analysis of an Antibody Recognizing
571 All Influenza A Subtypes." *Cell* 166 (3): 596–608.
572 <https://doi.org/10.1016/j.cell.2016.05.073>.
- 573 Kang, Xiaoping, Yuchang Li, Li Fan, Fang Lin, Jingjing Wei, Xiaolei Zhu, Yi Hu, Jing Li,
574 Guohui Chang, and Qingyu Zhu. 2012. "Development of an ELISA-Array for
575 Simultaneous Detection of Five Encephalitis Viruses." *Virology Journal* 9 (1): 56.
576 <https://doi.org/10.1186/1743-422X-9-56>.
- 577 Katzelnick, Leah C., Lionel Gresh, M. Elizabeth Halloran, Juan Carlos Mercado, Guillermina
578 Kuan, Aubree Gordon, Angel Balmaseda, and Eva Harris. 2017. "Antibody-Dependent
579 Enhancement of Severe Dengue Disease in Humans." *Science* 358 (6365): 929–32.
580 <https://doi.org/10.1126/science.aan6836>.
- 581 Kim, Hanbi, Doo-Ryeon Chung, and Minhee Kang. 2019. "A New Point-of-Care Test for the
582 Diagnosis of Infectious Diseases Based on Multiplex Lateral Flow Immunoassays."
583 *Analyst* 144 (8): 2460–66. <https://doi.org/10.1039/C8AN02295J>.
- 584 Kingsmore, Stephen F. 2006. "Multiplexed Protein Measurement: Technologies and
585 Applications of Protein and Antibody Arrays." *Nature Reviews Drug Discovery* 5 (4):
586 310. <https://doi.org/10.1038/nrd2006>.
- 587 Koopmans, M., Erwin de Bruin, G.-J. Godeke, I. Friesema, R. Van Gageldonk, Maarten
588 Schipper, Adam Meijer, Rob van Binnendijk, G. F. Rimmelzwaan, and M. D. De Jong.
589 2012. "Profiling of Humoral Immune Responses to Influenza Viruses by Using Protein
590 Microarray." *Clinical Microbiology and Infection* 18 (8): 797–807.
591 <https://doi.org/10.1111/j.1469-0691.2011.03701.x>.
- 592 Liew, Michael, Matthew C. Groll, James E. Thompson, Sara L. Call, Joann E. Moser, Justin D.
593 Hoopes, Karl Voelkerding, Carl Wittwer, and Rex S. Spendlove. 2007. "Validating a
594 Custom Multiplex ELISA against Individual Commercial Immunoassays Using Clinical
595 Samples." *Biotechniques* 42 (3): 327–33. <https://doi.org/10.2144/000112332>.
- 596 Lowell, George H., Sagit Ziv, Svetlana Bruzil, Ron Babecoff, and Tamar Ben-Yedidia. 2017.
597 "Back to the Future: Immunization with M-001 Prior to Trivalent Influenza Vaccine in

- 598 2011/12 Enhanced Protective Immune Responses against 2014/15 Epidemic Strain.”
599 *Vaccine* 35 (5): 713–15. <https://doi.org/10.1016/j.vaccine.2016.12.063>.
- 600 Madore, Dace V., Bruce D. Meade, Fran Rubin, Carolyn Deal, and Freyja Lynn. 2010.
601 “Utilization of Serologic Assays to Support Efficacy of Vaccines in Nonclinical and
602 Clinical Trials: Meeting at the Crossroads.” *Vaccine* 28 (29): 4539–47.
603 <https://doi.org/10.1016/j.vaccine.2010.04.094>.
- 604 Memoli, Matthew J., Pamela A. Shaw, Alison Han, Lindsay Czajkowski, Susan Reed, Rani
605 Athota, Tyler Bristol, Sarah Fargis, Kyle Risos, and John H. Powers. 2016. “Evaluation
606 of Antihemagglutinin and Antineuraminidase Antibodies as Correlates of Protection in an
607 Influenza A/H1N1 Virus Healthy Human Challenge Model.” *MBio* 7 (2): e00417-16.
608 <https://doi.org/10.1128/mBio.00417-16>.
- 609 Mendoza, Leo G., P. McQuary, A. Mongan, Rajeswari Gangadharan, Stafford Brignac, and
610 Maren Eggers. 1999. “High-Throughput Microarray-Based Enzyme-Linked
611 Immunosorbent Assay (ELISA).” *Biotechniques* 27 (4): 778–88.
612 <https://doi.org/10.2144/99274rr01>.
- 613 Nakajima, Rie, Medalyn Supnet, Algis Jasinskas, Aarti Jain, Omid Taghavian, Joshua Obiero,
614 Donald K. Milton, Wilbur H. Chen, Michael Grantham, and Richard Webby. 2018.
615 “Protein Microarray Analysis of the Specificity and Cross-Reactivity of Influenza Virus
616 Hemagglutinin-Specific Antibodies.” *MSphere* 3 (6): e00592-18.
617 <https://doi.org/10.1128/mSphere.00592-18>.
- 618 Price, Jordan V., Justin A. Jarrell, David Furman, Nicole H. Kattah, Evan Newell, Cornelia L.
619 Dekker, Mark M. Davis, and Paul J. Utz. 2013. “Characterization of Influenza Vaccine
620 Immunogenicity Using Influenza Antigen Microarrays.” *PloS One* 8 (5): e64555.
621 <https://doi.org/10.1371/journal.pone.0064555>.
- 622 Salazar, Georgina, Ningyan Zhang, Tong-Ming Fu, and Zhiqiang An. 2017. “Antibody
623 Therapies for the Prevention and Treatment of Viral Infections.” *Npj Vaccines* 2: 19.
624 <https://doi.org/10.1038/s41541-017-0019-3>.
- 625 Semenova, V. A., E. Steward-Clark, K. L. Stamey, T. H. Taylor, D. S. Schmidt, S. K. Martin, N.
626 Marano, and C. P. Quinn. 2004. “Mass Value Assignment of Total and Subclass
627 Immunoglobulin G in a Human Standard Anthrax Reference Serum.” *Clin. Diagn. Lab.*
628 *Immunol.* 11 (5): 919–23. <https://doi.org/10.1128/CDLI.11.5.919-923.2004>.
- 629 Templin, Markus F., Dieter Stoll, Monika Schrenk, Petra C. Traub, Christian F. Vöhringer, and
630 Thomas O. Joos. 2002. “Protein Microarray Technology.” *Drug Discovery Today* 7 (15):
631 815–22. [https://doi.org/10.1016/S1359-6446\(00\)01910-2](https://doi.org/10.1016/S1359-6446(00)01910-2).
- 632 Tighe, Patrick J., Richard R. Ryder, Ian Todd, and Lucy C. Fairclough. 2015. “ELISA in the
633 Multiplex Era: Potentials and Pitfalls.” *PROTEOMICS–Clinical Applications* 9 (3–4):
634 406–22. <https://doi.org/10.1002/prca.201400130>.
- 635 Urusov, Alexandr E., Anatoly V. Zherdev, and Boris B. Dzantiev. 2019. “Towards Lateral Flow
636 Quantitative Assays: Detection Approaches.” *Biosensors* 9 (3): 89.
637 <https://doi.org/10.3390/bios9030089>.
- 638 Wang, D., Y. Zheng, X. Kang, X. Zhang, H. Hao, W. Chen, L. Liu, X. Li, L. Li, and Q. Yuan.
639 2015. “A Multiplex ELISA-Based Protein Array for Screening Diagnostic Antigens and
640 Diagnosis of Flaviviridae Infection.” *European Journal of Clinical Microbiology &*
641 *Infectious Diseases* 34 (7): 1327–36. <https://doi.org/10.1007/s10096-015-2353-6>.
- 642 Yoshida, Taketoshi, Henrik Mei, Thomas Dörner, Falk Hiepe, Andreas Radbruch, Simon
643 Fillatreau, and Bimba F. Hoyer. 2010. “Memory B and Memory Plasma Cells.”

644 *Immunological Reviews* 237 (1): 117–39. <https://doi.org/10.1111/j.1600->
645 065X.2010.00938.
646

Figure 1. The ELISA-Array print pattern.

bioRxiv preprint doi: <https://doi.org/10.1101/2019.12.20.885285>; this version posted December 30, 2019. The copyright holder for this preprint (which was not certified by peer review) is the author/funder. All rights reserved. No reuse allowed without permission.

- 1: xIgG Fc (positive control)
- 2: HA H1 (group I)
- 3: HA H2 (group I)
- 4: HA H5 (group I)
- 5: FlulLaval vaccine (2018)
- 6: HA H3 (group II)
- 7: HA H7 (group II)
- 8: HA FluB (B/Yamagata)
- 9: HA FluB (B/Victoria)
- 10: GFP foldon (negative control)
- 11: xkappa biotin (fiducials)

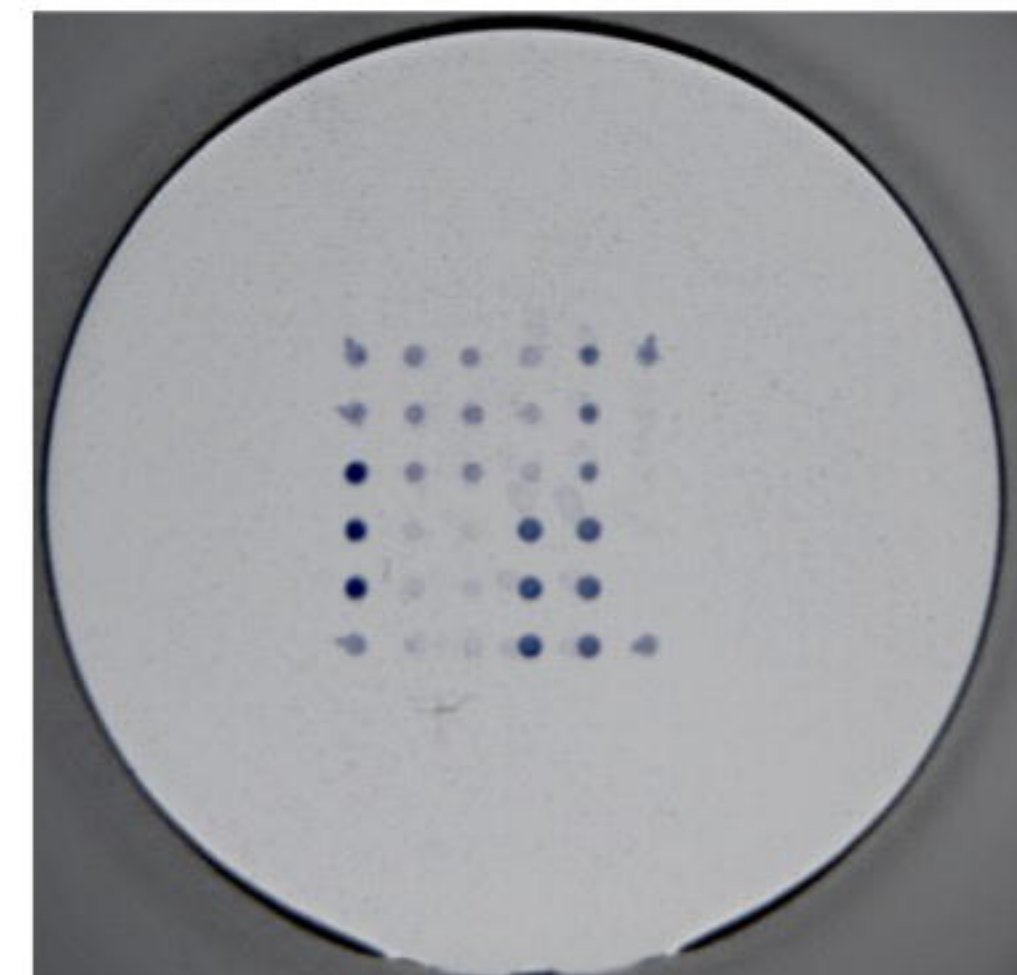


Figure 2. A comparison of the amount of protein needed in ELISA *versus* ELISA-Array.

bioRxiv preprint doi: <https://doi.org/10.1101/2019.12.20.885285>; this version posted December 30, 2019. The copyright holder for this preprint (which was not certified by peer review) is the author/funder. All rights reserved. No reuse allowed without permission.

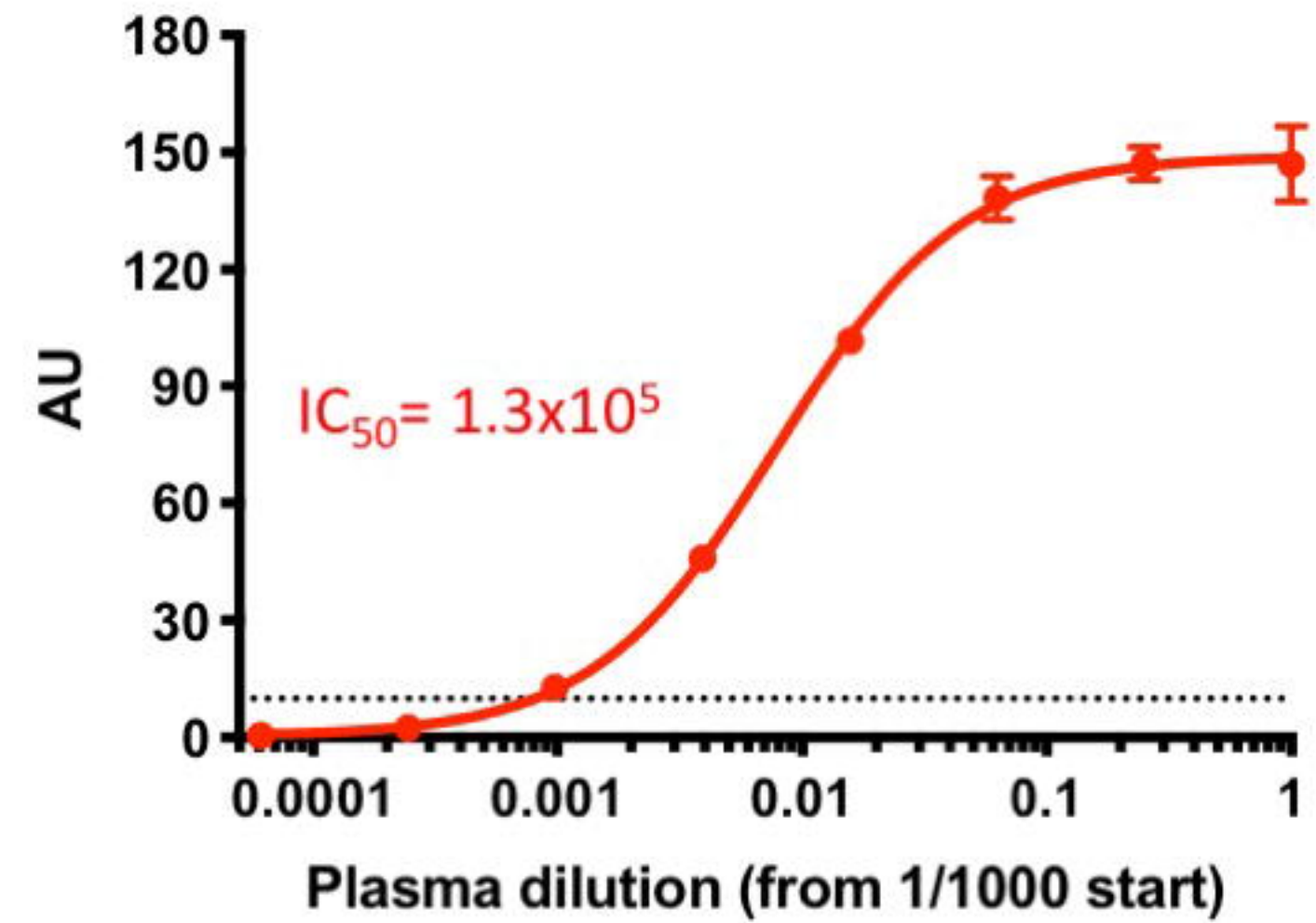
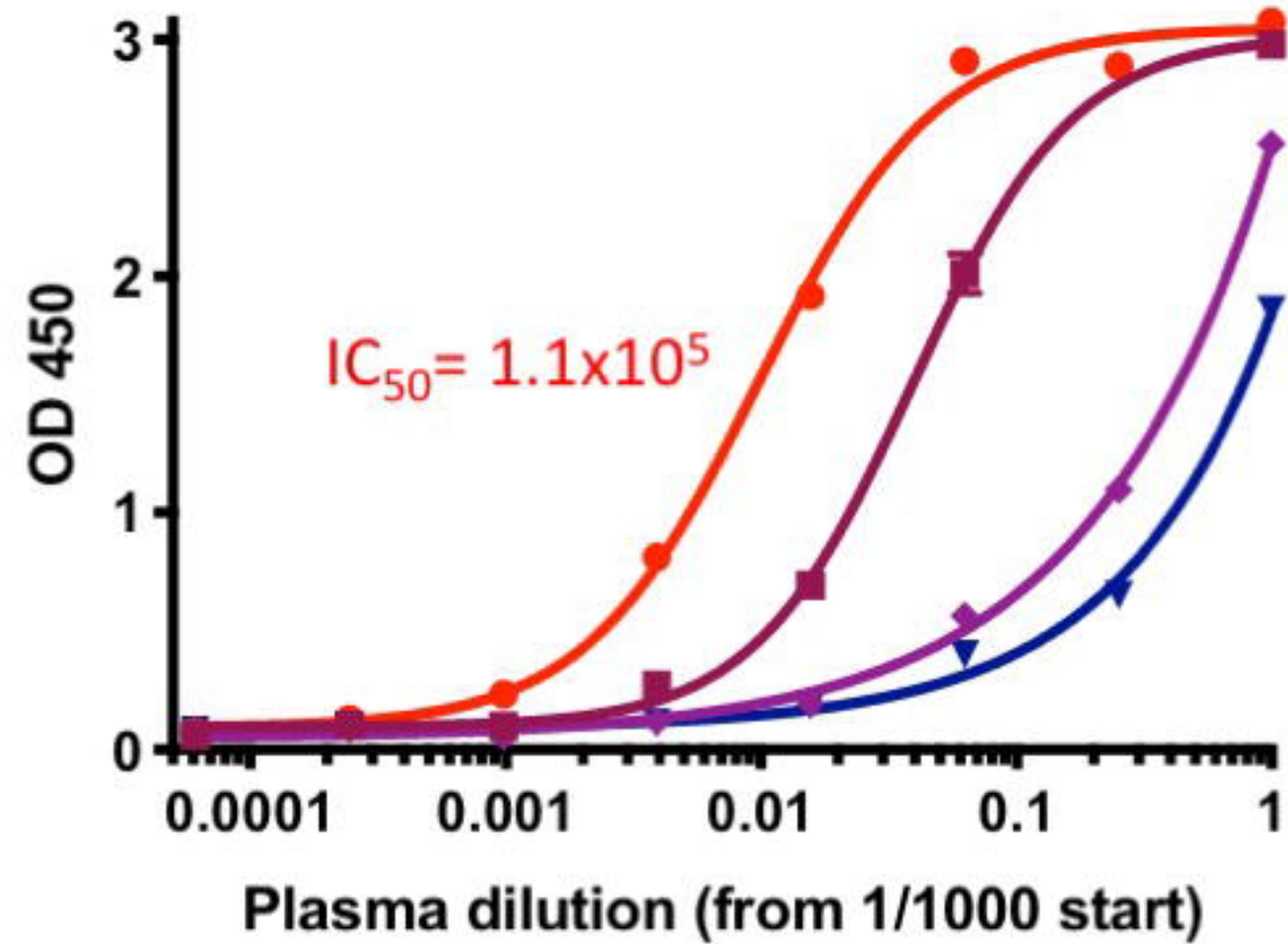


Figure 3. The sensitivity of the ELISA-Array.

bioRxiv preprint doi: <https://doi.org/10.1101/2019.12.20.885285>; this version posted December 30, 2019. The copyright holder for this preprint (which was not certified by peer review) is the author/funder. All rights reserved. No reuse allowed without permission.

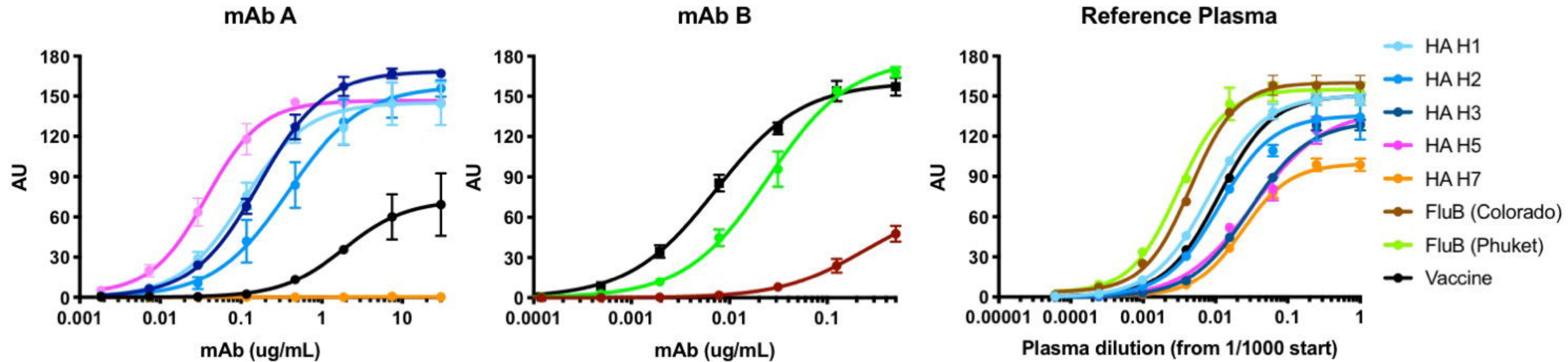


Figure 4. Dose-response curves of 3 donors on the Influenza antigen array.

bioRxiv preprint doi: <https://doi.org/10.1101/2019.12.20.885285>; this version posted December 30, 2019. The copyright holder for this preprint (which was not certified by peer review) is the author/funder. All rights reserved. No reuse allowed without permission.

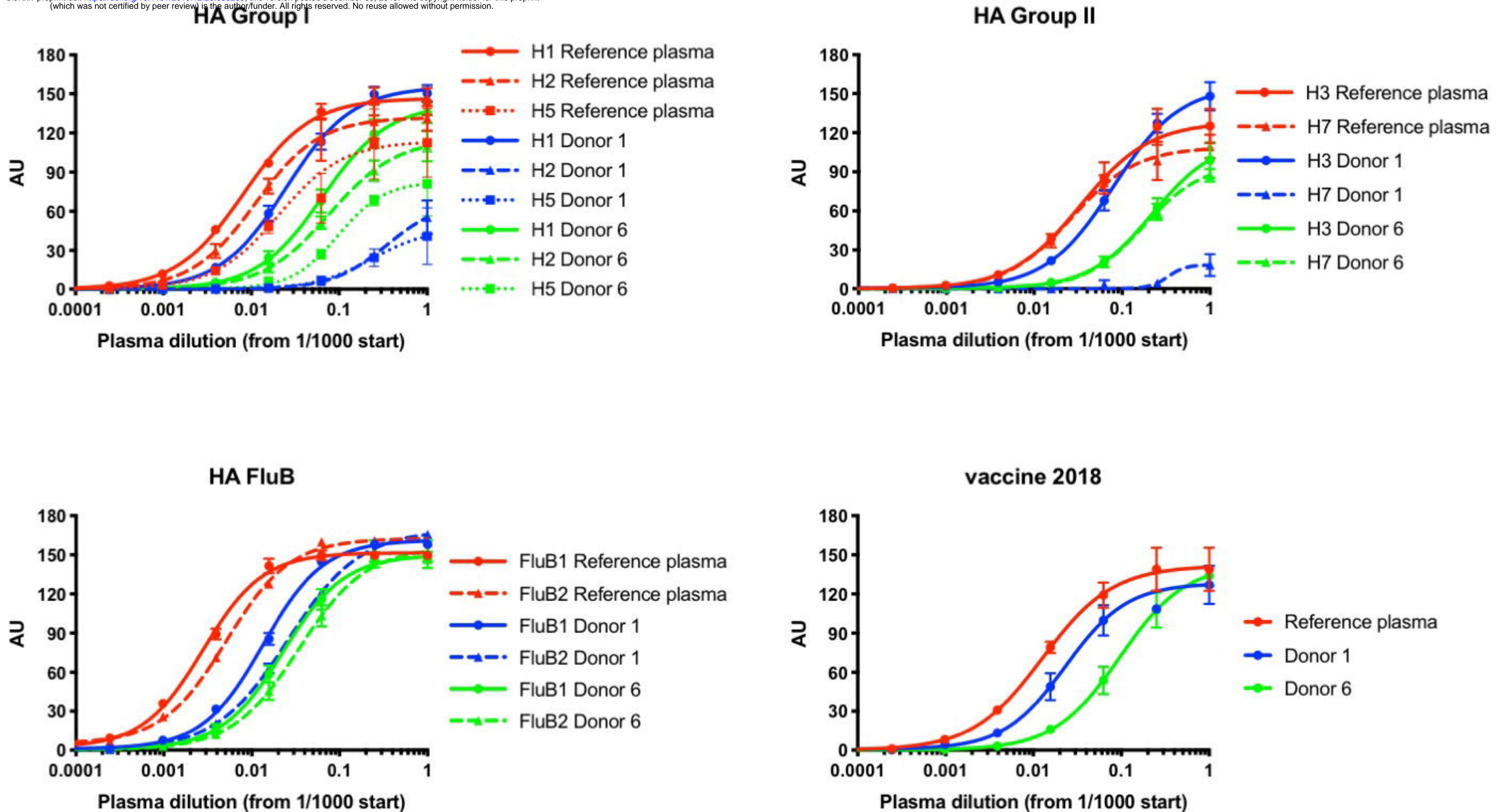


Figure 5. IC₅₀ comparisons of 3 donors on the Influenza antigen array.

bioRxiv preprint doi: <https://doi.org/10.1101/2019.12.20.885285>; this version posted December 30, 2019. The copyright holder for this preprint (which was not certified by peer review) is the author/funder. All rights reserved. No reuse allowed without permission.

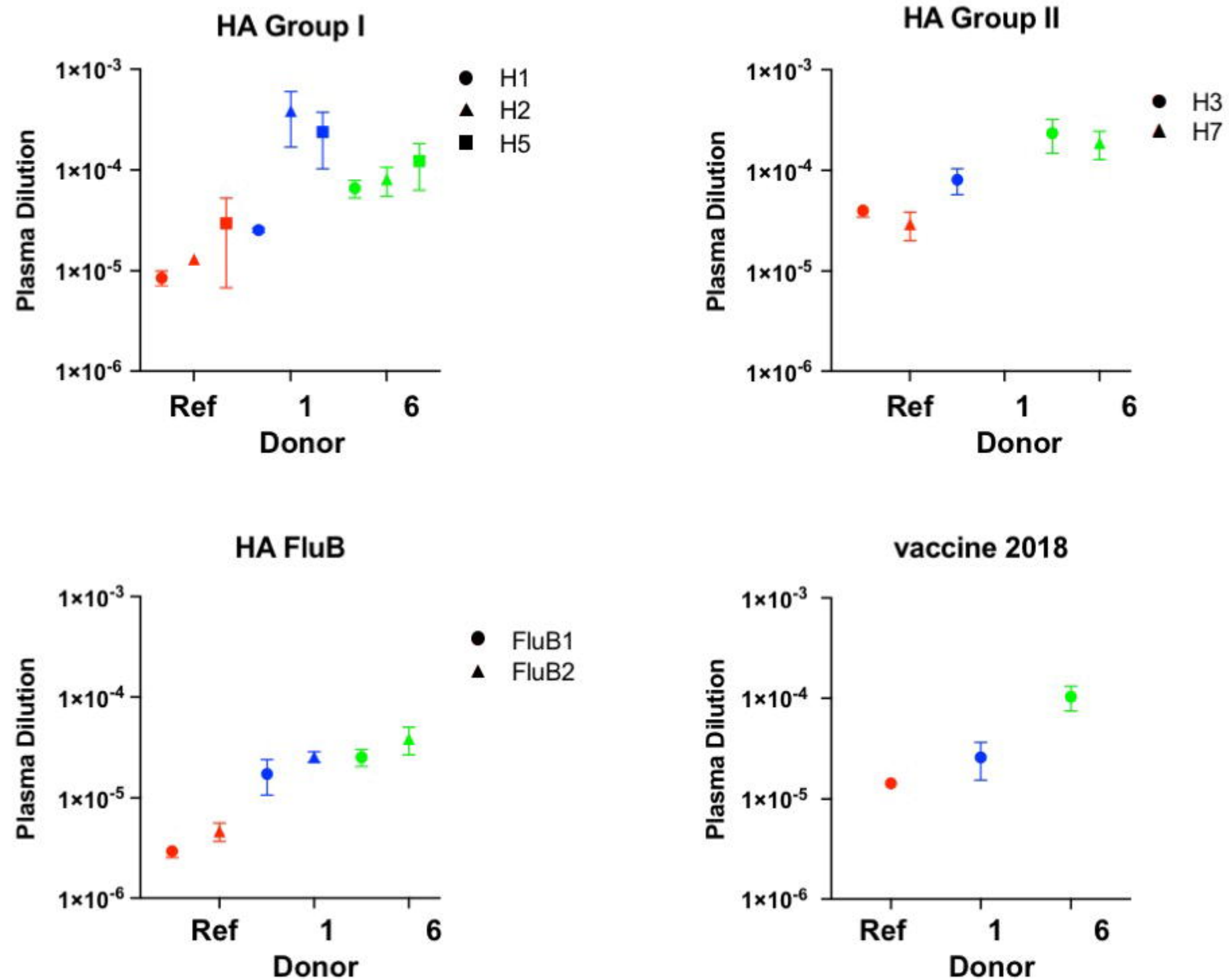
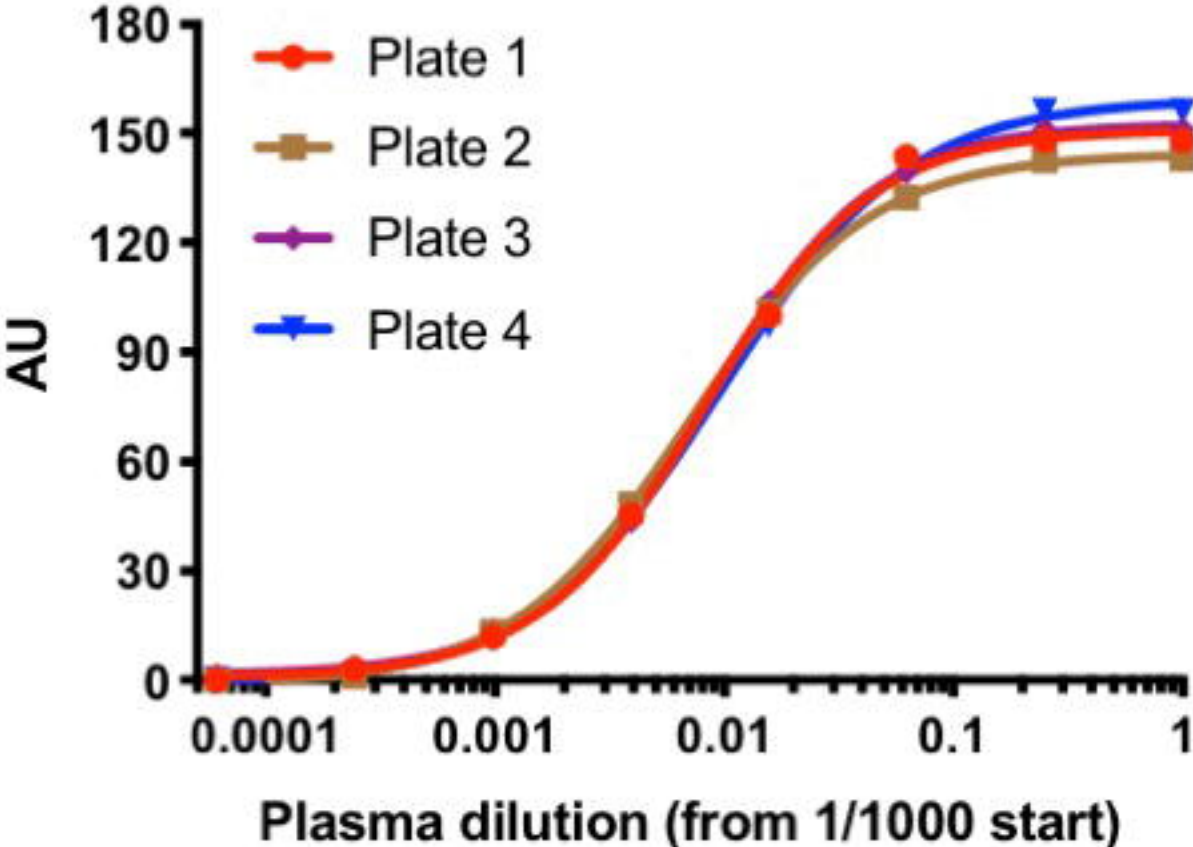


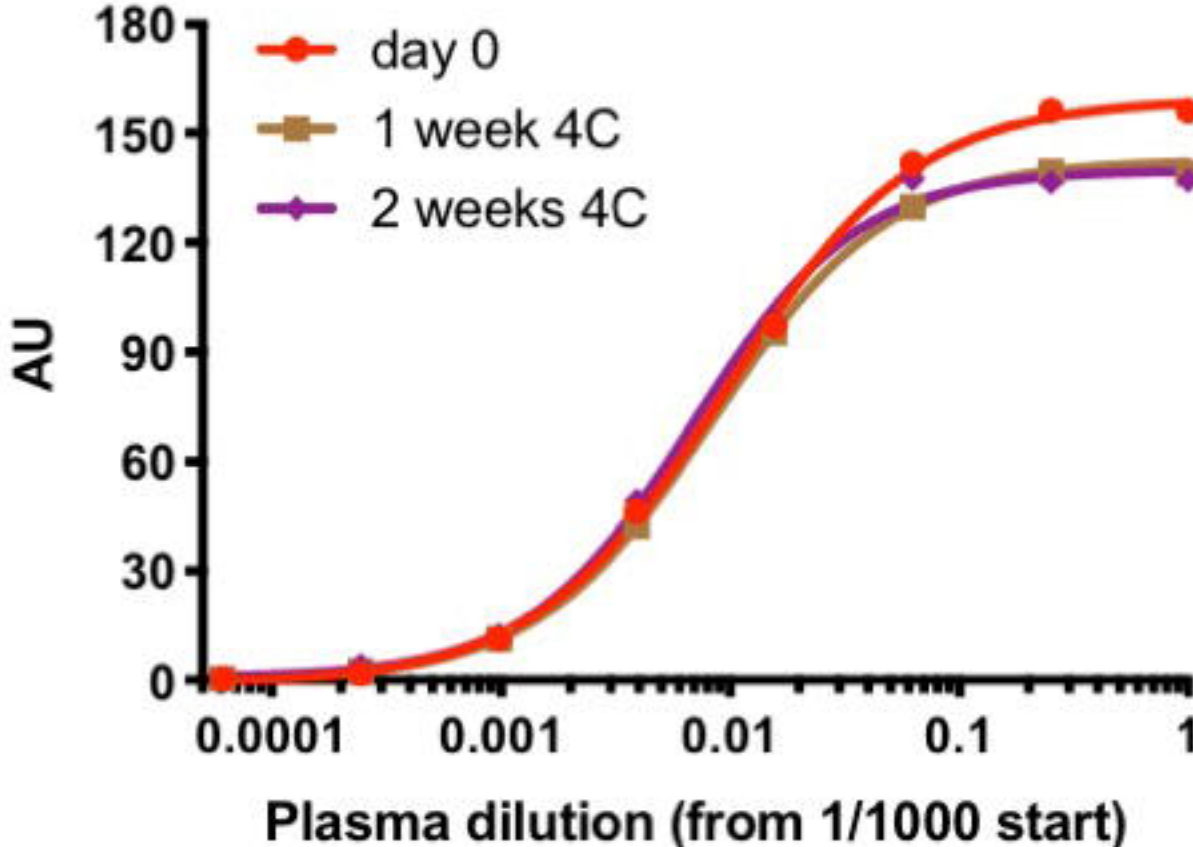
Figure 6. Intra-assay, Inter-assay and Stability Performance of the ELISA-Array.

bioRxiv preprint doi: <https://doi.org/10.1101/2019.12.20.885285>; this version posted December 30, 2019. The copyright holder for this preprint (which was not certified by peer review) is the author/funder. All rights reserved. No reuse allowed without permission.

Intra-assay



Inter-assay



Stability

